

Modulation of Pairing Symmetry with Bond Disorder in Unconventional Superconductors

Yao-Tai Kang,¹ Wei-Feng Tsai,^{2,1,*} and Dao-Xin Yao^{1,†}

¹State Key Laboratory of Optoelectronic Materials and Technologies,
School of Physics, Sun Yat-Sen University, Guangzhou 510275, China

²Department of Physics, National Sun Yat-sen University, Kaohsiung 80424, Taiwan

We study a two-orbital t - J_1 - J_2 model, originally developed to describe iron-based superconductors at low energies, in the presence of bond disorder (via next nearest-neighbor J_2 -bond dilution). By using Bogoliubov-de Gennes approach, we self-consistently calculate the local pairing amplitudes and the corresponding density of states, which demonstrate a change of dominant pairing symmetry from s_{\pm} -wave to d -wave when increasing disorder strength as long as $J_1 \lesssim J_2$. Moreover, the combined pairing interaction and strong bond disorder lead to the formation of s_{\pm} -wave “islands” with length scale of the superconducting coherence length embedded in a d -wave “sea”. This picture is further complemented by the disorder-averaged pair-pair correlation functions, distinct from the case with potential disorder, where the “sea” is insulating. Due to this inevitable formation of spatial inhomogeneity, the superconducting T_c determined by the superfluid density $\rho_s(T)$ obviously deviates the predicted value by the conventional Abrikosov-Gorkov theory, where the pairing amplitudes are viewed as uniformly suppressed as the disorder increases.

I. INTRODUCTION

Studying disorder effects in superconductors (SCs) is usually beneficial, though not in a direct manner, for unveiling their underlying pairing mechanism. An economic early indicator of the unconventional nature for a superconductor, for instance, can be the sensitivity of the superconducting transition temperature (T_c) to an amount of finite disorder.^{1–5} In addition, most unconventional SCs, such as cuprates⁶ and iron-based SCs^{7–9}, become superconducting after doping, which naturally introduces certain types of disorder in the materials. These materials are often complicated in composition and are intermediately or strongly coupled systems, causing a rather complex phase diagram with intertwined orders in which disorder might play a role.¹⁰ With substantial amounts of disorder, a SC may even undergo a zero-temperature quantum phase transition to another superconducting phase with distinct pairing symmetry^{11–15} or to a non-superconducting one.^{16,17}

From modeling point of view, a real disorder environment in a system may be simulated by either adding random one-body or many-body interactions. Both types of interactions include the variations of either amplitude or phase and can be further classified by the interaction range, *i.e.*, short range or long range. For instance, in Zn-doped cuprates like $\text{YBa}_2(\text{Cu}_{1-x}\text{Zn}_x)_3\text{O}_{6.9}$ such a disorder effect could be represented by a random set of scalar impurity potentials with a finite range.¹⁸ In fact, disorder effects resulting from random one-body potentials in SCs are widely discussed,^{18–21} while, in contrast, those from random many-body interactions are relatively less studied in a systematic way.^{22–26}

The discovery of iron-based SCs has enriched the unconventional SC physics in several aspects. One particularly interesting aspect is that the isovalent doping in both 1111 and 122 materials, which is theoretically pre-

dicted not to change electron density significantly,^{27–29} can suppress the stripe antiferromagnetic (AFM) order in the parent compounds.^{30,31} Moreover, it even induces superconductivity after intermediate doping in 122 materials;^{32,33} in some cases, there have been observed nodal structures in the superconducting gap,^{34–38} distinct from the fully gapped one upon charge doping. These findings may provide a possible playground to study random many-body interactions in SCs through the following intuition, provided the strong coupling picture is used.³⁹ For instance, a common consensus in $\text{BaFe}_2(\text{As}_{1-x}\text{P}_x)_2$ is that both magnetism and superconductivity should occur in FeAs plane, at which Fe atoms themselves form a square lattice with As atoms sitting above and below each plaquette center of the lattice alternately. Assuming that the stripe AFM order arises from the competition between nearest-neighbor (NN) J_1 and next nearest-neighbor (NNN) J_2 exchange interactions on the square lattice, the (random) substitution of As by P could result in two leading effects to disorder the system: one is to mainly suppress NNN J_2 exchange interactions and the other is to introduce a scalar potential at each plaquette center.

Thus, motivated by the experiments done in isovalent-doping iron-based SCs, we study the effects of purely exchange-interaction disorder (random J_2 -bond dilution, see Sec. II for the definition), from “weak” to “strong” (*i.e.*, x from 0 to 1), in a two-dimensional (2D), two-orbital t - J_1 - J_2 model.^{39,40} Although this model is originally developed to describe the low-energy physics of iron-based SCs, we simply consider a relatively ideal situation, make our study to be a topic of broad interest, but do not intend to claim it directly applicable to a certain real material.

When the bond disorder is “strong” with $0 \ll x < 1$ in a SC with short coherence length ξ , the standard theories for dirty SCs, valid as long as the electron mean free path $l \gg \xi > k_F^{-1}$, by Anderson¹ and by Abrikosov

and Gorkov² (AG) are expected to be insufficient to account for the disorder effects. Therefore, we address these issues by using self-consistent Bogoliubov-de Gennes formulation with the emphasis of the spatial inhomogeneity for the pairing amplitudes. Significantly, we find that: 1) As $J_1 \lesssim J_2$, the pairing symmetry of our model at zero-temperature ($T = 0$) is modulated from $s_{x^2y^2}$ -wave to $d_{x^2-y^2}$ -wave symmetry when the “disorder strength” x becomes greater than x_c ; this phenomenon is further confirmed by showing the electron density of states as a function of x . 2) The $T = 0$ spectral gap E_{gap} decreases following the same trend of the position/disorder averaged pairing amplitudes, $\bar{\Delta}_{s_{x^2y^2}}$ and $\bar{\Delta}_{d_{x^2-y^2}}$, as x grows. 3) When x is large, the combined pairing interaction and the J_2 -bond dilution disorder lead to the formation of $s_{x^2y^2}$ -wave “islands” of length scale $\mathcal{O}(\xi)$ embedded in a $d_{x^2-y^2}$ -wave “sea”; this picture is complemented by the disorder-averaged pair-pair correlation functions. 4) Due to this inevitable formation of spatial inhomogeneity, the superconducting T_c determined by the superfluid density $\rho_s(T)$ obviously deviates the predicted value by the AG theory, where the pairing amplitudes are viewed as uniformly suppressed as the disorder increases.

The rest of the paper is organized as follows. In Sec. II, we describe our model Hamiltonian and briefly sketch the numerical method we used. We then demonstrate our numerical results in Sec. III to show the modulation of the pairing symmetry with bond disorder. Several disorder-dependent physical quantities are presented to assist the understanding for this type of disorder, such as local pairing amplitudes, density of states, spectral gap, superfluid density and so on. In Sec. IV, we repeat all the calculations in Sec. III by taking away all J_1 exchange interactions to sharpen the effects due to J_2 -bond dilution. Finally, we conclude our findings in terms of a few remarks and a summary.

II. MODEL AND SELF-CONSISTENT BDG THEORY

Our adopted model Hamiltonian to capture the low-energy physics in *clean* iron-based superconductors is the so-called t - J_1 - J_2 model developed in Ref. 39, which has been further justified by functional renormalization group study.⁴¹ Explicitly, $H = H_0 + H_{int}$ and the non-interacting part reads

$$H_0 = \sum_{\mathbf{r}\mathbf{r}'} \sum_{\alpha\beta} \sum_{\sigma} \left(t_{\mathbf{r}\mathbf{r}'}^{\alpha\beta} c_{\mathbf{r}\alpha\sigma}^\dagger c_{\mathbf{r}'\beta\sigma} + h.c. \right) - \mu \sum_{\mathbf{r}\alpha} n_{\mathbf{r}\alpha}, \quad (1)$$

where $c_{\mathbf{r}\alpha\sigma}^\dagger$ ($c_{\mathbf{r}\alpha\sigma}$) creates (annihilates) an electron of α -orbital with spin σ ($\alpha = 1, 2$ for two degenerate “ d_{xz} ” and “ d_{yz} ” orbitals, respectively) at site \mathbf{r} . $n_{\mathbf{r}\alpha}$ is the local electron density operators with spin polarization α .

The normal-state Fermi surfaces in the unfolded Brillouin zone (one-iron per unit cell) can be reasonably

produced by setting $t_{\mathbf{r},\mathbf{r}+\hat{x}}^{11} = t_{\mathbf{r},\mathbf{r}+\hat{y}}^{22} = -1.0$, $t_{\mathbf{r},\mathbf{r}+\hat{x}}^{22} = t_{\mathbf{r},\mathbf{r}+\hat{y}}^{11} = 1.3$, $t_{\mathbf{r},\mathbf{r}+\hat{x}\pm\hat{y}}^{11/22} = -0.85$, $t_{\mathbf{r},\mathbf{r}+\hat{x}-\hat{y}}^{12/21} = t_{\mathbf{r},\mathbf{r}+\hat{x}+\hat{y}}^{21/12} = 0.85$, and other hopping parameters as zero, where \hat{x} and \hat{y} are unit vectors along the axes. For simplicity, we will take $|t_{\mathbf{r},\mathbf{r}+\hat{x}}^{11}| = 1$ as our energy units, lattice constant $a \equiv 1$, and set chemical potential $\mu = 1.8$, corresponding to electron density $n_e \approx 2.18$.

The interacting part includes several terms as follows,

$$H_{int} = \sum_{\langle\mathbf{r}\mathbf{r}'\rangle} \sum_{\alpha} J_1(\mathbf{r},\mathbf{r}') (\mathbf{S}_{\mathbf{r}\alpha} \cdot \mathbf{S}_{\mathbf{r}'\alpha} - n_{\mathbf{r}\alpha} n_{\mathbf{r}'\alpha}) + \sum_{\langle\langle\mathbf{r}\mathbf{r}'\rangle\rangle} \sum_{\alpha} J_2(\mathbf{r},\mathbf{r}') (\mathbf{S}_{\mathbf{r}\alpha} \cdot \mathbf{S}_{\mathbf{r}'\alpha} - n_{\mathbf{r}\alpha} n_{\mathbf{r}'\alpha}) + \dots, \quad (2)$$

where $\mathbf{S}_{\mathbf{r}\alpha} = c_{\mathbf{r},\alpha,\sigma}^\dagger \vec{\sigma}_{\sigma\sigma'} c_{\mathbf{r},\alpha,\sigma'}$ and $n_{\mathbf{r}\alpha}$ are the local spin and density operators with orbital index $\alpha = 1, 2$. $\langle\mathbf{r}\mathbf{r}'\rangle$ and $\langle\langle\mathbf{r}\mathbf{r}'\rangle\rangle$ denote NN and NNN pairs of sites, respectively, and thus the first two terms represent intra-orbital exchange interactions. In addition, “...” represent our ignored inter-orbital exchange and Hund’s coupling terms, which are shown to be unimportant on determining the pairing symmetry of the SC state in this model.

On a square lattice with $N = N_x \times N_y$ sites, the exchange couplings $J_2(\mathbf{r},\mathbf{r}')$ are taken to be zero when the (diagonal) bonds ($\mathbf{r}\mathbf{r}'$) cross the randomly selected xN plaquettes. In this way we introduce the “disorder” into our otherwise clean system. This kind of bond disorder is a quantum analog of bond-dilute Ising models^{42,43} while is rarely considered in superconducting systems. Physically, these selected plaquettes might represent the situation where the central atoms As are isovalently replaced by the atoms P, causing strong suppression of J_2 bonds in plaquettes. For simplicity, we further assume that the exchange couplings $J_1(\mathbf{r},\mathbf{r}') = J_1$ are unaffected. More delicate choice for $J_1(\mathbf{r},\mathbf{r}')$ will be discussed later.

Following Ref. 39, we assume that the superconductivity of the system can be reliably captured by mean-field approximation as long as the exchange interactions are small compared to the bandwidth ($\sim 12|t_1|$). The most dominant SC order parameters in our study would generally have the following symmetry form factor: $\Delta_\alpha = a_\alpha \cos k_x \cos k_y - (-1)^\alpha b_\alpha (\cos k_x - \cos k_y)$. The relative sign between $a_1(b_1)$ and $a_2(b_2)$ determines which irreducible representation the pairing symmetry belongs to, namely, A_{1g} for the plus sign and B_{1g} for the minus sign, given D_{4h} point group symmetry of our model. In the presence of disorder, we define the (local) real-space pairing amplitude for each orbital α as,

$$\Delta_\alpha(\mathbf{r},\mathbf{r}+\delta) = -J_l(\mathbf{r},\mathbf{r}+\delta) \langle c_{\mathbf{r},\alpha,\downarrow} c_{\mathbf{r}+\delta,\alpha,\uparrow} \rangle \quad (3)$$

with $\delta = \pm\hat{x}, \pm\hat{y}$ for NN pairing ($l = 1$), and $\delta = \pm\hat{x} \pm \hat{y}$ for NNN pairing ($l = 2$). The mean-field Hamiltonian of

H is then written as

$$H^{MF} = H_0 + \sum_{\mathbf{r}, \delta, \alpha} \Delta_{\alpha}^*(\mathbf{r}, \mathbf{r} + \delta) c_{\mathbf{r}, \alpha, \downarrow} c_{\mathbf{r} + \delta, \alpha, \uparrow} + h.c. \quad (4)$$

Within BdG formalism, we diagonalize the *quadratic*, mean-field Hamiltonian (4) through the BdG equation,

$$\begin{pmatrix} \hat{K}_{\mathbf{r}\alpha\mathbf{r}'\beta} & \hat{\Delta}_{\alpha\beta} \\ \hat{\Delta}_{\alpha\beta}^* & -\hat{K}_{\mathbf{r}\alpha\mathbf{r}'\beta}^* \end{pmatrix} \begin{pmatrix} u_{\mathbf{r}'\beta}^n \\ v_{\mathbf{r}'\beta}^n \end{pmatrix} = E_n \begin{pmatrix} u_{\mathbf{r}\alpha}^n \\ v_{\mathbf{r}\alpha}^n \end{pmatrix}, \quad (5)$$

with $\hat{K}_{\mathbf{r}\alpha\mathbf{r}'\beta} = -t_{\mathbf{r}\alpha\mathbf{r}'\beta} - \mu\delta_{\mathbf{r}\mathbf{r}'}\delta_{\alpha\beta}$. The relation between Bogoliubov quasi-particle operators γ and electron operators is $c_{\mathbf{r}\alpha\sigma} = \sum_n (u_{\mathbf{r}\alpha}^n \gamma_{n\sigma} - \sigma v_{\mathbf{r}\alpha}^{n*} \gamma_{n\bar{\sigma}}^\dagger)$, and hence combining with the definition, for instance, of s -wave $\cos k_x \cdot \cos k_y$ SC order parameter, this gives rise to the following self-consistent conditions,

$$\Delta_{\alpha}(\mathbf{r}, \mathbf{r} + \delta) = \frac{1}{2} \sum_n J_2(\mathbf{r}, \mathbf{r} + \delta) \tanh \frac{E_n}{2k_B T} \times (u_{\mathbf{r}, \alpha}^n v_{\mathbf{r} + \delta, \alpha}^{n*} + v_{\mathbf{r}, \alpha}^{n*} u_{\mathbf{r} + \delta, \alpha}^n), \quad (6)$$

and

$$\begin{aligned} \langle n_{\alpha, \mathbf{r}} \rangle &= \langle c_{\mathbf{r}\alpha}^\dagger c_{\mathbf{r}\alpha} \rangle \\ &= \sum_n |v_{\mathbf{r}\alpha}^n|^2 [1 - f(E_n)] + \sum_n |u_{\mathbf{r}\alpha}^n|^2 f(E_n), \end{aligned} \quad (7)$$

where $f(E)$ is the Fermi distribution function. We have studied the model for a few sets of J_1, J_2 (values in a clean system), and a wide range of isovalent doping percentage $0 < x < 1$ on square lattices of sizes up to $N = 32 \times 32$. We always perform our computations on a finite lattice sites with periodic boundary conditions. For a given (quenched) disorder configuration, we obtain the resultant quasi-particle spectrum by repeatedly diagonalizing BdG Eq. (5) after each iteration of the pairing amplitudes according to self-consistency conditions (6) and (7) until sufficient accuracy is achieved (*e.g.*, the relative error of the pairing amplitudes is less than 0.01%).

III. MODULATION OF PAIRING SYMMETRY WITH BOND DISORDER

A. Pairing symmetry and local pairing amplitudes

The zero-temperature phase diagram of t - J_1 - J_2 model in the context of iron-based superconductors has been well studied in the clean limit, $x = 0$.^{39,44} There are four spatial symmetries for the singlet pairing by decoupling J_1 and J_2 interactions: $s_{x^2y^2}$, $s_{x^2+y^2}$, $d_{x^2-y^2}$, and d_{xy} . Given the two-orbital nature of our model and D_{4h} point group symmetry (when taking one iron per unit cell), every spatial symmetry may even belong to different irreducible representations. For instance, one can have $s_{x^2y^2}^{A_{1g}}$ (also called s_{\pm} -wave) and $s_{x^2y^2}^{B_{1g}}$, or $d_{x^2-y^2}^{A_{1g}}$ and $d_{x^2-y^2}^{B_{1g}}$.

In the presence of disorder ($x \neq 0$), the pairing am-

plitudes could be no longer uniform and are likely to be inhomogeneous in a self-consistent manner. Therefore, we define the intra-orbital spin-singlet pairing amplitude on an NN bond as (similar for an NNN bond pairing)

$$\Delta_{\alpha}(\mathbf{r}, \mathbf{r} + \delta) = -\frac{J_1}{2} \langle c_{\mathbf{r}, \alpha, \downarrow} c_{\mathbf{r} + \delta, \alpha, \uparrow} - c_{\mathbf{r}, \alpha, \uparrow} c_{\mathbf{r} + \delta, \alpha, \downarrow} \rangle, \quad (8)$$

and three dominant local pairing amplitudes with appropriate pairing symmetries all in A_{1g} irreducible representation,

$$\begin{aligned} \Delta_{s_{x^2y^2}}(\mathbf{r}) &= \frac{1}{8} \sum_{\alpha\delta'} \Delta_{\alpha}(\mathbf{r}, \mathbf{r} + \delta'), \\ \Delta_{s_{x^2+y^2}}(\mathbf{r}) &= \frac{1}{8} \sum_{\alpha\delta} \Delta_{\alpha}(\mathbf{r}, \mathbf{r} + \delta), \\ \Delta_{d_{x^2-y^2}}(\mathbf{r}) &= \frac{1}{8} \sum_{\alpha} [\Delta_{\alpha}(\mathbf{r}, \mathbf{r} + \hat{x}) - \Delta_{\alpha}(\mathbf{r}, \mathbf{r} + \hat{y}) \\ &\quad + \Delta_{\alpha}(\mathbf{r}, \mathbf{r} - \hat{x}) - \Delta_{\alpha}(\mathbf{r}, \mathbf{r} - \hat{y})], \end{aligned} \quad (9)$$

where $\delta = \pm\hat{x}, \pm\hat{y}$ and $\delta' = \pm\hat{x} \pm \hat{y}$. When determining which pairing symmetry is most dominant for a given disorder proportion x , we take an average over the whole lattice positions and disorder configurations for each local pairing amplitudes shown in Eq. (9).

To consider the effects of the bond disorder, we first plot the zero-temperature x vs. J_1 phase diagram in Fig. 1(a) with corresponding averaged pairing amplitudes in Fig. 1(b), where J_2 is fixed to be $|t_1|$. One of the most important observations is that as long as $J_1 \lesssim J_2$, the pairing symmetry of the superconducting ground state would be modulated from a s_{\pm} -wave to a d -wave pairing symmetry when the disorder x grows greater than certain critical x_c ; on the contrary, as $J_1 \gtrsim J_2$ the d -wave symmetry would dominate no matter what x is.

Note that all the phases appear in the phase diagram belong to A_{1g} irreducible representation. Thus, in a strict sense, there should be no sharp phase transitions in our disordered system. The crossover boundary between phases, the green line, represents the degeneracy of the averaged pairing amplitudes between the *dominant* $s_{x^2y^2}^{A_{1g}}$ and $d_{x^2-y^2}^{A_{1g}}$ symmetries, while the dashed line represents the *subdominant* line between $s_{x^2y^2}^{A_{1g}}$ and $s_{x^2+y^2}^{A_{1g}}$ symmetries, as shown in Fig. 1(b). The pairing amplitudes belonging to B_{1g} irreducible representation always have a smaller weight than those of A_{1g} 's. So, every pairing symmetry in this work will refer to A_{1g} irreducible representation and we will omit the superscript hereafter.

When $x = 0$ (1), the pairing amplitudes for various pairing symmetry channels are *uniform* with $\Delta_{s_{x^2y^2}}(\mathbf{r}) = 0.1585 > \Delta_{d_{x^2-y^2}}(\mathbf{r}) = 0.0991$ ($\Delta_{d_{x^2-y^2}}(\mathbf{r}) = 0.0194 > \Delta_{s_{x^2+y^2}}(\mathbf{r}) = 0.0049$), given $J_1 = 0.7$ and $J_2 = 1$ in the system. But, as we have mentioned earlier in this subsection, the pairing amplitudes are not necessary to be so when $0 < x < 1$. In Figs. 2(a)-(c), we provide a statistical distribution of the local pairing amplitudes $P(|\Delta(\mathbf{r})|)$ for several disorder x in different pairing symmetry channels

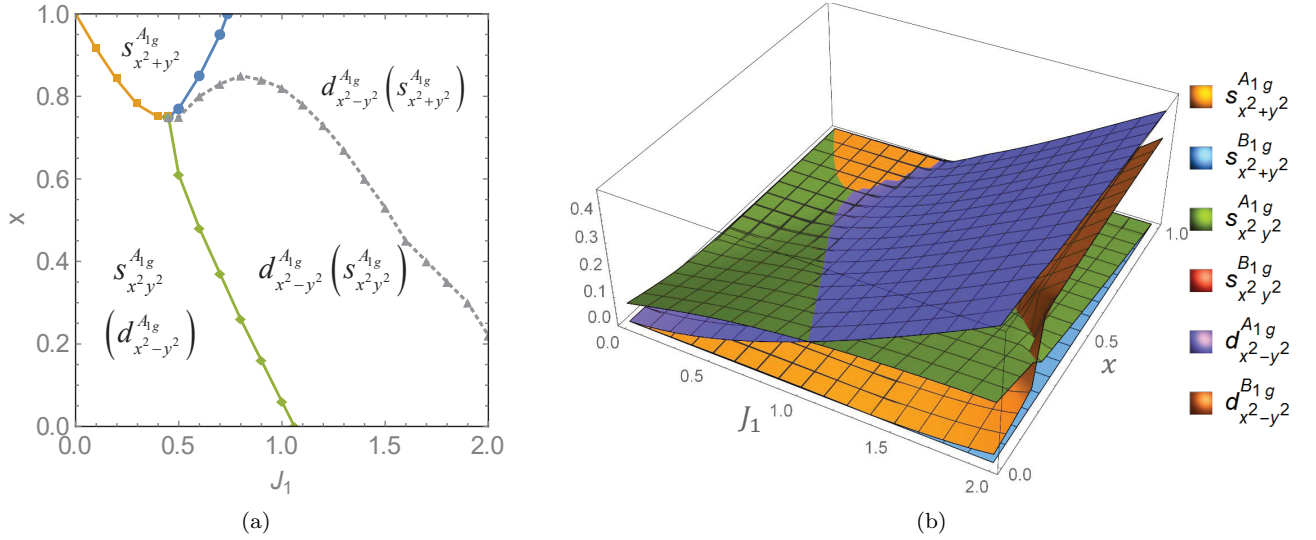


FIG. 1. (a) Schematic zero-temperature phase diagram as a function of J_1 and disorder x , given $J_2 = |t_1|$ on a 32×32 square lattice. The green line marks the boundary between the dominant $d_{x^2-y^2}^{A_{1g}}$ -wave pairing region and $s_{x^2-y^2}^{A_{1g}}$ -wave pairing one, while the dashed line marks the boundary between subdominant $s_{x^2-y^2}^{A_{1g}}$ -wave pairing region and $s_{x^2+y^2}^{A_{1g}}$ -wave pairing one; the subdominant pairing symmetries are shown within the brackets. (b) The position and disorder averaged pairing amplitudes for each pairing symmetry as a function of J_1 and x .

at zero temperature. When $x = 0.1$ or $x = 0.9$, each distribution function shows a major sharp peak, indicating the uniformity of the system. As x grows from 0.1, the major peak becomes lower and broader ($|\Delta|$ are spread in a wider range of values), indicating the non-uniformity of the system which reaches its maximum at $x = 0.5$. Further increasing x , the distribution is basically reversed and the amplitudes become more uniform again.

The behavior we found here as x increases is qualitatively similar to that seen in a usual s -wave superconductor from weak to strong site-impurity disorder.²⁰ (AG theory breaks down!) However, there exists a sharp feature never seen in the simple site-impurity case: For $s_{x^2-y^2}$ -wave pairing symmetry [see Fig. 2(b)], the distribution function shows a few extra sub-peaks except for the major one for every given x . This is a unique property which distinguishes $s_{x^2-y^2}$ -wave pairing from the other two pairing channels [see Figs. 2(a) and 2(c)]. In fact, this feature may be physically understood as follows. First, the $s_{x^2-y^2}$ -wave pairing originates from J_2 exchange term, not from J_1 term. Second, since the disorder is introduced by randomly taking away the NNN (J_2) bonds, there should be five different local disorder configurations, as illustrated in Fig. 2(d). Therefore, in a macroscopic system, all the five configurations should in principle be reflected on the distribution function in terms of the peaks observed in Fig. 2(b). (Sometimes the distribution peak corresponding to either the configuration I or V is too small to be seen.)

B. Density of states and energy gap

One simple way to demonstrate a possible modulation of pairing symmetry as x increases is to calculate the electron density of states (DOS), which is expressed as

$$N(\omega) = \frac{1}{N} \sum_{\mathbf{r}\alpha n} [|u_{\mathbf{r}\alpha}^n|^2 \delta(E_n - \omega) + |v_{\mathbf{r}\alpha}^n|^2 \delta(E_n + \omega)], \quad (10)$$

where the delta function has the form of Cauchy-Lorentz distribution function, $\delta(x) = \gamma/\pi(x^2 + \gamma^2)$, with an infinitesimal scale parameter $\gamma = 0.008$.

Fig. 3 shows the DOS for different x at zero temperature in a 56×56 lattice. Each data curve is obtained by averaging over the whole lattice positions as well as 30 disorder configurations at any given x . With increasing disorder x , the superconducting gap around $\omega = 0$ decreases and evolves from U-shape like to more V-shape like, indicating a modulation of the pairing symmetry from $s_{x^2-y^2}$ -wave to $d_{x^2-y^2}$ -wave. In addition, the coherence peaks are slowly smeared out, behaving similarly to the case with impurity disorder.²⁰

The evolution of the gap in the DOS result may be complemented by the quasi-particle energy gap E_{gap} , which is defined as the smallest positive eigenvalue of the BdG Hamiltonian in Eq. (5). As shown in Fig. 4, E_{gap} decreases when x increases and it also evolves in the same trend as (position and disorder averaged) $\overline{\Delta}_{s_{x^2-y^2}}$; otherwise, if there were no $\Delta_{s_{x^2-y^2}}$ component in the SC state, E_{gap} should be ideally zero due to nodal quasi-

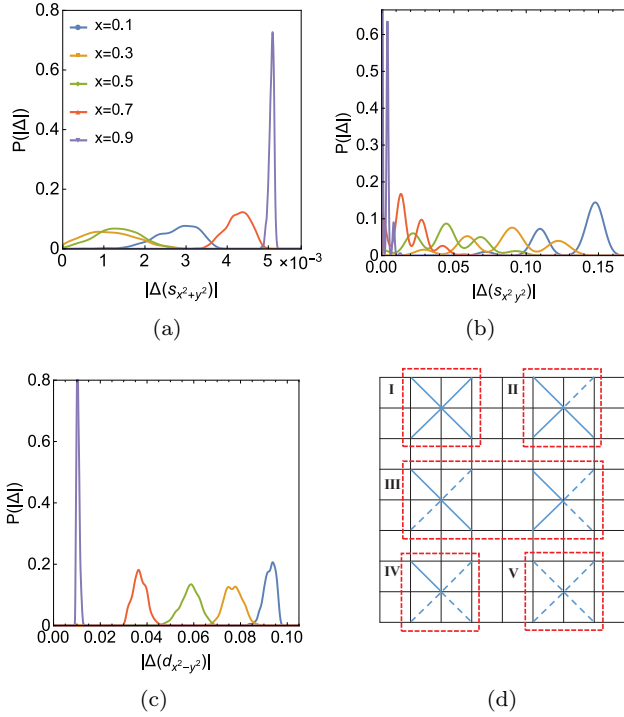


FIG. 2. Distribution of the local pairing amplitudes $P(|\Delta(\mathbf{r})|)$ for various disorder x at zero temperature, with $J_1 = 0.7$ and $J_2 = 1$. (a), (b) and (c) correspond to $s_{x^2+y^2}$ -, $s_{x^2y^2}$ -, and $d_{x^2-y^2}$ -wave pairing amplitudes, respectively. (d) Five possible disordered configurations for a local lattice site. The dashed lines denote the NNN bond-defect ($J_2 = 0$).

particle excitations from d -wave pairing. Note that when $x \gtrsim 0.75$, E_{gap} is slightly greater than $\overline{\Delta}_{s_{x^2+y^2}}$, which is due to the presence of $\overline{\Delta}_{s_{x^2+y^2}}$ in the system (not shown in Fig. 4). Therefore, E_{gap} appears to be dictated mainly by $\overline{\Delta}_{s_{x^2+y^2}}$ in a certain way. The subtle feature of it could be further revealed by the physics we will discuss next.

C. Formation of superconducting clusters

In our study, local pairing amplitudes are self-consistently calculated at every lattice site by using BdG theory for a given disorder realization. In particular, as mentioned in subsection III A, the distribution of $s_{x^2y^2}$ -wave pairing amplitudes seems to be correlated with local disorder configurations. Usually this should be contrasted with the electron density distribution. Therefore, in Figs. 5(a), 5(b), and 5(d), we plot the electron density $n(\mathbf{r}) = \sum_{\alpha\sigma} \langle n_{\alpha,\mathbf{r},\sigma} \rangle$ and spatial variation of $s_{x^2y^2}$ -wave and $d_{x^2-y^2}$ -wave pairing amplitudes, respectively, for a given disorder realization with $x = 0.8$ at zero temperature. Obviously, the electron density $n(\mathbf{r})$ is nearly homogeneous and uncorrelated with the given bond disorder. However, the $s_{x^2y^2}$ -wave pairing amplitudes are inhomogeneous and tend to form some s -wave SC “islands” on

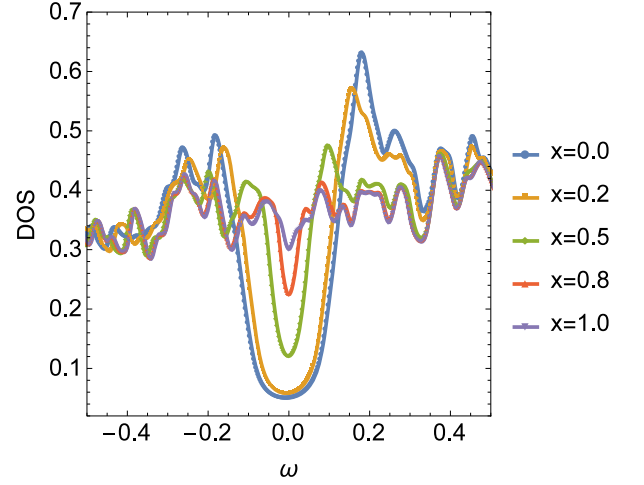


FIG. 3. Density of states for various disorder proportions x at zero temperature, with $J_1 = 0.7$ and $J_2 = 1$. Each DOS for a given x has been averaged over position and 30 disorder configurations.

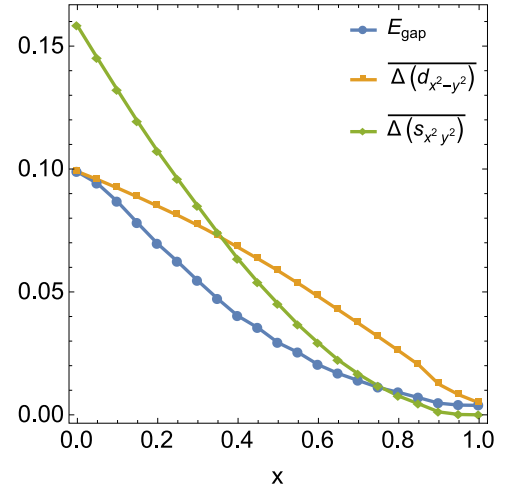


FIG. 4. Quasi-particle gap E_{gap} and position/disorder averaged pairing amplitudes $\overline{\Delta}_{s_{x^2+y^2}}$, $\overline{\Delta}_{s_{x^2y^2}}$ and $\overline{\Delta}_{d_{x^2-y^2}}$ as a function of x with $J_1 = 0.7$ and $J_2 = 1$.

top of a relatively less inhomogeneous d -wave SC “sea”, even though there is no intrinsic correlation between disordered bonds. Note that there is also a small clustering tendency for $d_{x^2-y^2}$ -wave pairing amplitudes, which is likely to be induced by s -wave piece.

To further confirm the formation of s -wave SC “islands” without a strong correlation with a certain disorder configuration, we display the disorder-averaged correlation functions $\overline{\Delta}(\mathbf{r}_1)\overline{\Delta}(\mathbf{r}_2)$ for $s_{x^2y^2}$ - and $d_{x^2-y^2}$ -wave pairing amplitudes as a function of the distance $r_{ij} = |\mathbf{r}_1 - \mathbf{r}_2|$ at $x = 0.8$ in Fig. 6(a). The s -wave component shows a clear structure on a scale of two to three lattice constants, while the d -wave counterpart shows almost no structure. Note that the coherence length in a

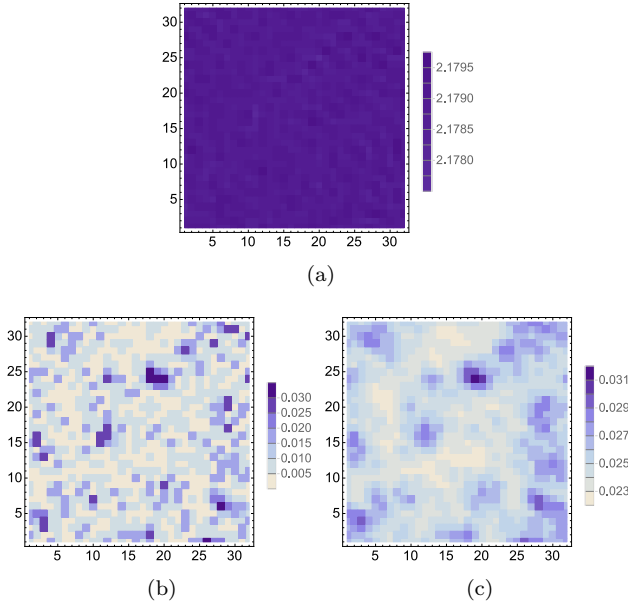


FIG. 5. (a) Electron density on a 32×32 lattice for a given disorder realization with $x = 0.8$ at zero temperature. (b) and (c) correspond to two dominant $s_{x^2-y^2}$ - and $d_{x^2-y^2}$ -wave pairing channels. The darker the larger density/amplitude would be.

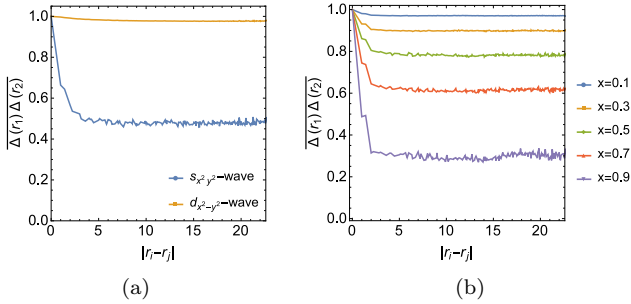


FIG. 6. (a) The disorder-averaged correlation functions $\overline{\Delta(\mathbf{r}_1)\Delta(\mathbf{r}_2)}$ for $s_{x^2-y^2}$ - and $d_{x^2-y^2}$ -wave pairing amplitudes as a function of the distance $r_{ij} = |\mathbf{r}_1 - \mathbf{r}_2|$ with $x = 0.8$. (b) $\overline{\Delta(\mathbf{r}_1)\Delta(\mathbf{r}_2)}$ of $s_{x^2-y^2}$ -wave pairing for various x . Both (a) and (b) are averaged over 15 random disorder configurations and both are scaled by $\overline{\Delta^2(\mathbf{r}_1)}$.

clean $s_{x^2-y^2}$ -wave SC in this model can be estimated by $v_F/\Delta \sim 4$. Moreover, the clustering tendency for the s -wave component persists as x increases as can be seen in Fig. 6(b).

Additionally, it is worth noticing that for the first few lowest quasi-particle excited states, each corresponding wave function distribution, $|\Psi(\mathbf{r})|^2$, appears to be a propagating mode with a definite momentum along the diagonal direction; along each wave front (e.g., of the largest amplitude), the probability distributes almost uniformly but suppresses around s -wave SC “islands”. Such variation in $|\Psi(\mathbf{r})|^2$ suggests its nature as a

gapped mode. Thus, this feature might well explain why $E_{gap} > 0$, as found in Fig. 4, is dictated by the s -wave pairing channel in our inhomogeneous SC system.

D. Superfluid density, Critical temperature, and Phase diagram

The temperature dependence of the superfluid density $\rho_s(T)$ is usually viewed as a good indicator to determine if a superconductor is “unconventional” or not. For instance, $\rho_s(T)$, which is measurable through the magnetic penetration depth $\lambda^{-2}(T)$, exhibits an exponential behavior in T in a clean (hole-doped) 122 compound, $\text{Ba}_{1-x}\text{K}_x\text{Fe}_2\text{As}_2$, suggesting a fully gapped SC;⁴⁵ while $\rho_s(T)$ behaves like a power law in an electron-doped $\text{Ba}(\text{Fe}_{1-x}\text{Co}_x)_2\text{As}_2$, indicating the presence of nodes or something unconventional.^{46–48}

Moreover, the qualitative behavior of $\rho_s(T)$ gives a useful hint to understand 1) how disorder of certain type may affect SC (phase rigidity) at low temperatures^{18,20} and 2) what type of fluctuations is essential near critical temperature T_c .⁴⁹ Although the answer to question 2) is beyond our mean-field study, we can still use it to obtain T_c in a self-consistent manner when inhomogeneous pairing is inevitable and not negligible.

We generalize the linear-response approach in Refs. 50 and 51 for a multi-orbital case to obtain the superfluid density. Considering a weak vector potential $A_x(\mathbf{r}, t)$ along x direction, the hopping terms in Eq. (1) are modified by the Peierls phase factors $-e^{ieA_x(\mathbf{r})}$. Expanding the phase factors up to second order, we obtain

$$H_t^A = H_t - \sum_{\mathbf{r}} \left[e j_x^p(\mathbf{r}) A_x(\mathbf{r}) + \frac{1}{2} e^2 k_x(\mathbf{r}) A_x^2(\mathbf{r}) \right], \quad (11)$$

with the paramagnetic current

$$j_x^p(\mathbf{r}) = i \sum_{s\sigma} \sum_{\alpha\beta} t_{\mathbf{r},\mathbf{r}+s}^{\alpha\beta} \left(c_{\mathbf{r}+s,\beta\sigma}^\dagger c_{\mathbf{r}\alpha\sigma} - c_{\mathbf{r}\alpha\sigma}^\dagger c_{\mathbf{r}+s,\beta\sigma} \right),$$

and the kinetic energy associated with x direction

$$k_x(\mathbf{r}) = - \sum_{s\sigma} \sum_{\alpha\beta} t_{\mathbf{r},\mathbf{r}+s}^{\alpha\beta} \left(c_{\mathbf{r}+s,\beta\sigma}^\dagger c_{\mathbf{r}\alpha\sigma} + c_{\mathbf{r}\alpha\sigma}^\dagger c_{\mathbf{r}+s,\beta\sigma} \right).$$

According to the linear response theory,

$$\rho_s = \langle -k_x \rangle - \Lambda_{xx}(q_x = 0, q_y \rightarrow 0, i\omega = 0), \quad (12)$$

where $\langle -k_x \rangle$ is the kinetic energy along x direction, and

$$\Lambda_{xx}(\mathbf{q}, i\omega_m) = \frac{1}{N^2} \int_0^\beta d\tau e^{i\omega_m \tau} \langle j_x^p(\mathbf{q}, \tau) j_x^p(-\mathbf{q}, 0) \rangle. \quad (13)$$

Note that in our disordered model, we calculate the

current-current correlation function in real space,

$$\Lambda_{xx}(\mathbf{r}_1, \mathbf{r}_2, i\omega_m) = \frac{1}{N} \int_0^\beta d\tau e^{i\omega_m \tau} \langle j_x^p(\mathbf{r}_1, \tau) j_x^p(\mathbf{r}_2, 0) \rangle. \quad (14)$$

After disorder averaging, the translational invariance may be recovered and hence we set $\Lambda_{xx}(\mathbf{r}_1, \mathbf{r}_2, i\omega) = \Lambda_{xx}(\mathbf{r}_1 - \mathbf{r}_2, i\omega)$, followed by a Fourier transform to \mathbf{q} -space,

$$\Lambda_{xx}(\mathbf{q}, i\omega) = \frac{1}{N^2} \sum_{\mathbf{r}_1 \mathbf{r}_2} e^{-i\mathbf{q} \cdot (\mathbf{r}_1 - \mathbf{r}_2)} \Lambda_{xx}(\mathbf{r}_1, \mathbf{r}_2, i\omega). \quad (15)$$

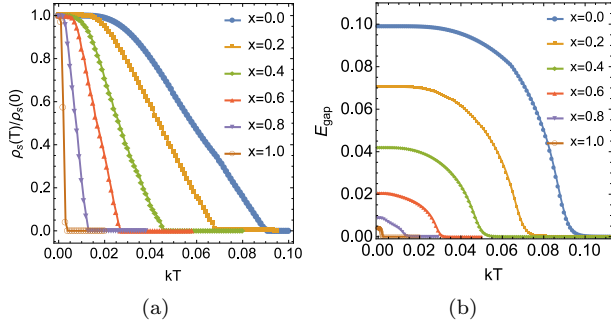


FIG. 7. (a) Temperature dependence of superfluid density $\rho_s(T)$ and energy gap E_{gap} for various disorder proportion x .

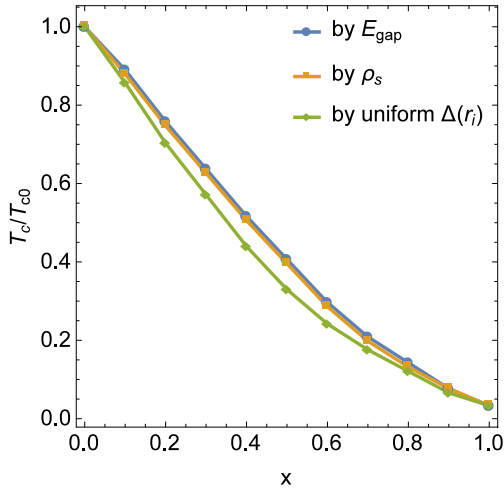


FIG. 8. Critical temperature T_c as a function of x , obtained by quasi-particle gap minimum E_{gap} , superfluid density ρ_s , and the AG-type calculation with enforced uniform $\Delta(\mathbf{r}_i)$, respectively.

In Fig. 8(a), we show the temperature dependence of $\rho_s(T)$, normalized by $\rho_s(0)$, at various x . At any given x , $\rho_s(T)$ deviates from $\rho_s(0)$ exponentially at low temperatures and then decreases until reaching zero at a critical T (called T_c). This can be contrasted by the minimum

quasi-particle energy E_{gap} as a function of T depicted in Fig. 8(b) with a similar trend. Such an exponential behavior strongly suggests the SC ground state of the system is fully gapped.

A few remarks are worth mentioning here. First, unlike in the case of site-impurity disorder, $\rho_s(0)$ is basically not suppressed as the disorder strength x increases, indicating that the phase coherence for electrons is almost unaffected. Second, at $x > x_c$ even though the d -wave component is dominant, there could be no gapless Bogoliubov quasi-particles, as indicated in Fig. 8(b) at $T < T_c$. Third, ' T_c 's determined by $\rho_s(T)$ and $E_{gap}(T)$ are not necessarily the same. In fact, E_{gap} usually overestimates T_c slightly in our study (see Fig. 8). This is because a system may have certain local pairing amplitudes while completely lose the phase coherence among them. Therefore, T_c determined by ρ_s would be more reliable.

Typically the standard AG theory provides an estimation of the suppressed T_c in a disordered superconductor. The suppressed T_c , ΔT , is basically proportional to the disorder scattering rate, $x/N(0)$, times a constant of $\mathcal{O}(1)$. The essential step in its derivation is to replace $\Delta(\mathbf{r})$ by the spatially averaged one. Therefore, we also calculate the quasi-particle gap with an enforced uniform order parameter $\Delta(\mathbf{r}_i)$ in the self-consistent mean-field equations and summarize all of our obtained T_c in Fig. 8. It is important to observe that E_{gap} -determined T_c via the inhomogeneous solution in the self-consistent manner agrees well with the ρ_s -determined one, but both are away from the AG-type T_c when $0 < x < 1$. This strongly implies the breakdown of the conventional AG-type theory for the bond-disordered system.

IV. SYSTEM WITHOUT J_1

We have studied a J_2 -bond disordered t - J_1 - J_2 model in the previous sections. However, the presence of J_1 terms may couple with J_2 terms in a complicated way and features purely from the bond disorder could be still obscure. Since this type of disorder is interesting on its own right, in this section, we repeat previous calculations by setting $J_1 = 0$.

Focusing on $s_{x^2y^2}$ -wave only, Fig. 9(b) shows the distribution of the spatial pairing amplitudes at zero temperature with its corresponding disorder realization at $x = 0.4$ depicted in Fig. 9(a). The trend to form "superconducting islands" is clear [see Figs. 9(c)→(b)→(d)]: As $x \gtrsim 0.5$, "Superconducting islands" are formed while gradually become smaller until x approaches 1. These "islands" are instead separated from one another by a metallic "sea" (with negligible $\Delta(\mathbf{r})$). This can be more accurately confirmed by the disorder-averaged correlation function $\overline{\Delta(\mathbf{r}_1)\Delta(\mathbf{r}_2)}$ for various x , as shown in Fig. 10.

We next examine the quasi-particle minimum gap E_{gap} as a function of the disorder proportion x at zero temperature, as illustrated in Fig. 11. Clearly, E_{gap} follows the

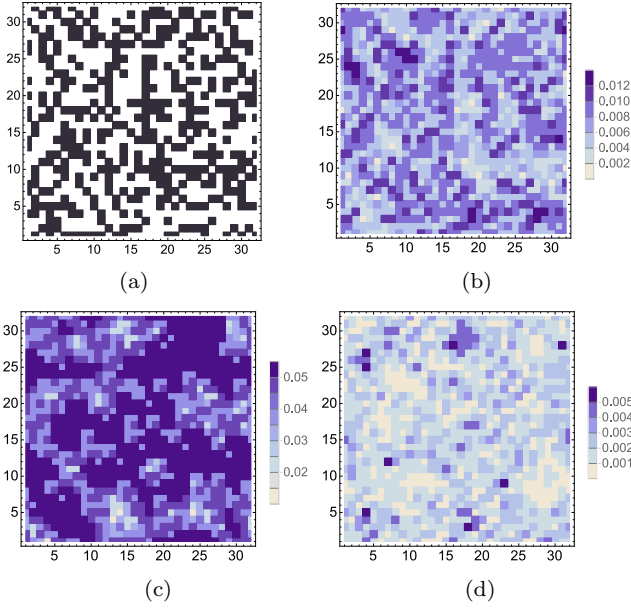


FIG. 9. (a) A disordered pattern with $x = 0.4$. The purple regions mark the points with $J_2 = 0$. (b) The spatial distribution of local pairing amplitudes corresponding to (a). The darker purple color indicates the regions with larger pairing amplitudes. (c) and (d) are another two spatial distributions of local pairing amplitudes with $x = 0.1$ and $x = 0.7$ respectively. The darker purple color has the same meaning explained in (b)

same trend as $\overline{\Delta}_{s_{x^2y^2}}$. Note that even though the system tends to form the “superconducting islands” as x grows, the superfluid stiffness ρ_s doesn’t vanish until $x = 1$ (See Fig. 12). This is because, within our BdG formalism, we ignored the possible phase fluctuations between SC islands, which can frustrate Cooper pairs to form a coherent superconducting state. Thus, in principle, one may not rule out the occurrence of a superconductor-metal transition in this purely academic model. Moreover, in Fig. 12 T_c determined by either E_{gap} or superfluid density ρ_s is consistent with each other; while AG-type calculation is again shown to underestimate T_c , reflecting on the importance of the inhomogeneous pairing amplitudes.

V. DISCUSSION AND CONCLUSION

Before concluding our work, there are a few additional remarks worth mentioning here, which are relevant to isovalent doping in iron-based SCs. Firstly, as we have mentioned in Sec. II, in the strong coupling picture the leading effect of the substitution of P for As reduces seriously the exchange interaction J_2 (presumably superexchange type). However, a number of subleading effects are also anticipated. For instance, one might consider to include the weakened NN exchange interaction J_1 and

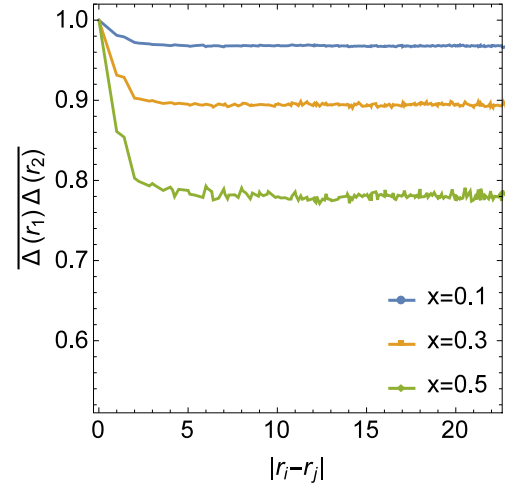


FIG. 10. The correlation function $\overline{\Delta(\mathbf{r}_1)\Delta(\mathbf{r}_2)}$ for $s_{x^2y^2}$ -pairing amplitudes as a function of the distance $r_{ij} = |\mathbf{r}_1 - \mathbf{r}_2|$ with different x , averaged by 15 configurations and scaled by $\Delta^2(\mathbf{r}_1)$.

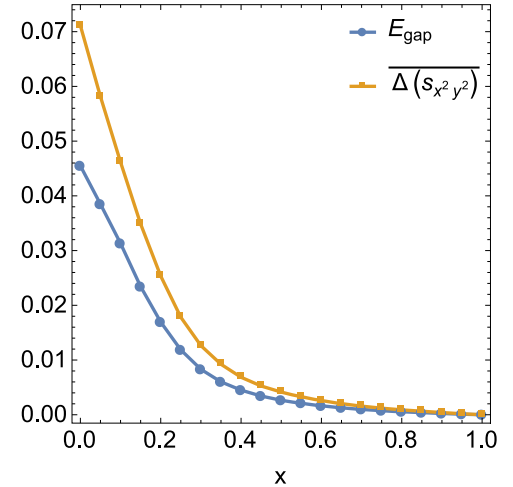


FIG. 11. The energy gap E_{gap} as a function of the disorder proportion x at zero temperature. With x raising, E_{gap} reduces gradually and reaches zero at $x = 1.0$.

the presence of short-range impurity potentials. Both of them are basically pair breakers: The former suppresses the d -wave superconductivity, while the latter could erase the phase information or even insulate originally superconducting regions. As long as the ratio of the impurity potential strength to J_1 is much less than one, our results shown in the previous sections may remain valid qualitatively.

Secondly, although our prediction on the modulation of the pairing symmetry may be applicable for the isovalent-doping 1111 iron-based SCs at finite temperatures, where $\text{LaOFeAs}_{1-x}\text{P}_x$ ($x = 1$) has been reported to have gap nodes,^{34,35} our theory cannot sufficiently describe 122

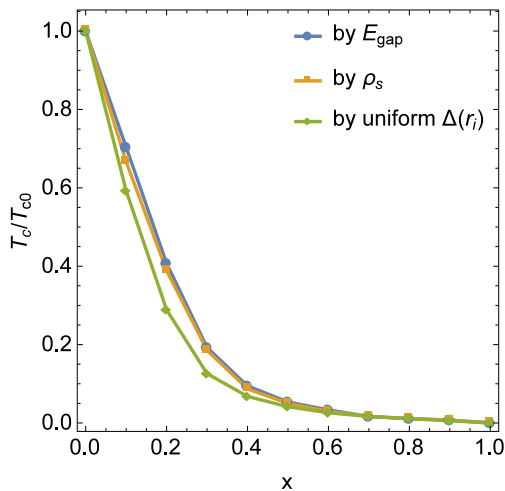


FIG. 12. Superconducting critical temperature T_c as a function of x , with $J_1 = 0, J_2 = 1$.

systems. This is because we have so far ignored the magnetic and orbital fluctuations, which are believed to play important roles in exhibiting either an antiferromagnetic order or a nematic state.²⁶ We will refer this more generic consideration to a future study.

In summary, we studied the bond disorder effects, from “weak” to “strong”, in an unconventional superconductor described by the two-orbital t - J_1 - J_2 model. We used self-consistent Bogoliubov-de Gennes formulation to em-

phasize the necessity of the spatial inhomogeneity for the pairing amplitudes. In particular, we found that as long as $J_1 \lesssim J_2$, the pairing symmetry of our model at $T = 0$ can be modulated from $s_{x^2y^2}$ -wave to $d_{x^2-y^2}$ -wave symmetry when the “disorder strength” x goes beyond x_c . This result was best presented by the electron density of states as a function of x and could be partially justified by any negative evidence in experiments about probing fully gapped s_{\pm} -wave order.^{52–54} Moreover, when x is large, we observed the formation of $s_{x^2y^2}$ -wave “islands” with length scale $\mathcal{O}(\xi)$ embedded in a $d_{x^2-y^2}$ -wave “sea”, due to the combined pairing interaction and the J_2 -bond disorder. As a consequence, T_c determined by the superfluid density $\rho_s(T)$ is found to deviate from the predicted value by the AG theory, suggesting its insufficiency to describe the bond disorder effects.

ACKNOWLEDGMENTS

We would like to acknowledge Fan Yang, Jiangping Hu and Elbio Dagotto for stimulating discussions. W.F.T. is supported in part by MOST in Taiwan under Grant No.103-2112-M-110-008-MY3 and the Thousand-Young-Talent Program of China. Y.T.K. and D.X.Y. acknowledge support from NBRPC-2012CB821400, NSFC-11574404, NSFC-11275279, NSFC-2015A030313176, NSFC-Guangdong Joint Fund and National Supercomputer Center in Guangzhou, Shanghai Forum, and Fundamental Research Funds for the Central Universities of China.

* weifengt@gmail.com

† yaodaos@mail.sysu.edu.cn

¹ P. W. Anderson, Phys. Rev. Lett. **3**, 325 (1959).

² A. A. Abrikosov and L. P. Gorkov, Zh. Eksp. Teor. Fiz. **39**, 1781 (1960) [Sov. Phys. JETP **12**, 1243 (1961)].

³ M. Sigrist and K. Ueda, Rev. Mod. Phys. **63**, 239 (1991).

⁴ A. V. Balatsky, I. Vekhter, and J.-X. Zhu, Rev. Mod. Phys. **78**, 373 (2006).

⁵ H. Alloul, J. Bobroff, M. Gabay, and P. J. Hirschfeld, Rev. Mod. Phys. **81**, 45 (2009).

⁶ For a recent summary, see B. Keimer, S. A. Kivelson, M. R. Norman, S. Uchida, and J. Zaanen, Nature **518**, 179 (2015).

⁷ G. R. Stewart, Rev. Mod. Phys. **83**, 1589 (2011).

⁸ P. Dai, J. Hu, and E. Dagotto, Nature Physics **8**, 709 (2012).

⁹ X. Chen, P. Dai, D. Feng, T. Xiang, and F.-C. Zhang, National Science Review **1**, 371 (2014).

¹⁰ E. Fradkin, S. A. Kivelson, and J. M. Tranquada, Rev. Mod. Phys. **87**, 457 (2015).

¹¹ Tai-Kai Ng, Phys. Rev. Lett. **103**, 236402 (2009).

¹² H. Kontani and S. Onari, Phys. Rev. Lett. **104**, 157001 (2010).

¹³ D. V. Efremov, M. M. Korshunov, O. V. Dolgov, A. A. Golubov, and P. J. Hirschfeld, Phys. Rev. B **84**, 180512(R) (2011).

(2011).

¹⁴ B. Spivak, P. Oreto, and S. A. Kivelson, Phys. Rev. B **77**, 214523 (2008).

¹⁵ B. Spivak, P. Oreto, and S. A. Kivelson, Physica B **404**, 462 (2009).

¹⁶ M. P. A. Fisher, Phys. Rev. Lett. **65**, 923 (1990).

¹⁷ Y. Dubi, Y. Meir, and Y. Avishai, Nature **449**, 876 (2007).

¹⁸ M. Franz, C. Kallin, A. J. Berlinsky, and M. I. Salkola, Phys. Rev. B **56**, 7882 (1997).

¹⁹ T. Xiang and J. M. Wheatley, Phys. Rev. B **51**, 11721 (1995).

²⁰ A. Ghosal, M. Randeria, N. Trivedi, Phys. Rev. B **65**, 014501 (2001).

²¹ H. Chen, Y.-Y. Tai, C. S. Ting, M. J. Graf, J. Dai, and J.-X. Zhu, Phys. Rev. B **88**, 184509 (2013).

²² In two dimensions, the interplay between localization and superconductivity due to certain types of disorder (including random many-body interactions), is usually represented by the disordered quantum XY model or Josephson-junction array model after integrating out all fermionic degrees of freedom.

²³ J. W. Halley, S. Davis, and S. Sen, Physica B: Condensed Matter **165**, 999 (1990).

²⁴ O. Parcollet and A. Georges, Phys. Rev. B **59**, 5341 (1999).

²⁵ J. Otsuki and D. Vollhardt, Phys. Rev. Lett. **110**, 196407 (2013).

- (2013).
- ²⁶ Shuhua Liang, Christopher B. Bishop, Adriana Moreo, Elbio Dagotto, Phys. Rev. B **92**, 104512 (2015).
 - ²⁷ A. I. Coldea, J. D. Fletcher, A. Carrington, J. G. Analytis, A. F. Bangura, J.-H. Chu, A. S. Erickson, I. R. Fisher, N. E. Hussey, and R. D. McDonald, Phys. Rev. Lett. **101**, 216402 (2008).
 - ²⁸ S. Kasahara, T. Shibauchi, K. Hashimoto, K. Ikada, S. Tonegawa, R. Okazaki, H. Shishido, H. Ikeda, H. Takeya, K. Hirata, T. Terashima and Y. Matsuda, Phys. Rev. B **81**, 184519 (2010).
 - ²⁹ F. Rullier-Albenque, D. Colson, A. Forget, P. Thury, and S. Poissonnet, Phys. Rev. B **81**, 224503 (2010).
 - ³⁰ C. de la Cruz, W. Z. Hu, S. Li, Q. Huang, J. W. Lynn, M. A. Green, G. F. Chen, N. L. Wang, H. A. Mook, Q. Si, and P. Dai, Phys. Rev. Lett. **104**, 017204 (2010).
 - ³¹ S. Kasahara, H. J. Shi, K. Hashimoto, S. Tonegawa, Y. Mizukami, T. Shibauchi, K. Sugimoto, T. Fukuda, T. Terashima, A. H. Nevidomskyy, and Y. Matsuda, Nature **486**, 382 (2012).
 - ³² S. Jiang, H. Xing, G. Xuan, C. Wang, Z. Ren, C. Feng, J. Dai, Z. Xu, and G. Cao, J. Phys.: Condens. Matter **21**, 382203 (2009).
 - ³³ Y. Nakai, T. Iye, S. Kitagawa, K. Ishida, H. Ikeda, S. Kasahara, H. Shishido, T. Shibauchi, Y. Matsuda, and T. Terashima, Phys. Rev. Lett. **105**, 107003 (2010).
 - ³⁴ J. D. Fletcher, A. Serafin, L. Malone, J. G. Analytis, J.-H. Chu, A. S. Erickson, I. R. Fisher, and A. Carrington, Phys. Rev. Lett. **102**, 147001 (2009).
 - ³⁵ C. W. Hicks, T. M. Lippman, M. E. Huber, J.G. Analytis, J. H. Chu, A. S. Erickson, I. R. Fisher, K. A. Moler, Phys. Rev. Lett. **103**, 127003 (2009).
 - ³⁶ K. Hashimoto, M. Yamashita, S. Kasahara, Y. Senshu, N. Nakata, S. Tonegawa, K. Ikada, A. Serafin, A. Carrington, T. Terashima, H. Ikeda, T. Shibauchi, and Y. Matsuda, Phys. Rev. B **81**, 220501(R) (2010).
 - ³⁷ Y. Nakai *et al.*, Phys. Rev. B **81**, 020503 (2010).
 - ³⁸ J. S. Kim, P. J. Hirschfeld, G. R. Stewart, S. Kasahara, T. Shibauchi, T. Terashima, and Y. Matsuda, Phys. Rev. B **81**, 214507 (2010).
 - ³⁹ K. Seo, B. A. Bernevig, and J. Hu, Phys. Rev. Lett. **101**, 206404 (2008).
 - ⁴⁰ Q. Si and E. Abrahams, Phys. Rev. Lett. **101**, 076401 (2008).
 - ⁴¹ H. Zhai, F. Wang, and D.-H. Lee, Phys. Rev. B **80**, 064517 (2009).
 - ⁴² D. Zoln, Phys. Rev. B **18**, 2387 (1978).
 - ⁴³ E. Mina, A. Bohorquez, Ligia E. Zamora, and G. A. Perez Alcazar, Phys. Rev. B **47**, 7925 (1993).
 - ⁴⁴ P. Goswami, P. Nikolic, and Q. Si, EPL **91**, 37006 (2010).
 - ⁴⁵ K. Hashimoto, T. Shibauchi, S. Kasahara, K. Ikada, S. Tonegawa, T. Kato, R. Okazaki, C. J. van der Beek, M. Konczykowski, H. Takeya, K. Hirata, T. Terashima, and Y. Matsuda, Phys. Rev. Lett. **102**, 207001 (2009).
 - ⁴⁶ R. T. Gordon, N. Ni, C. Martin, M. A. Tanatar, M. D. Vannette, H. Kim, G. D. Samolyuk, J. Schmalian, S. Nandi, A. Kreyssig, A. I. Goldman, J. Q. Yan, S. L. Budko, P. C. Canfield, and R. Prozorov, Phys. Rev. Lett. **102**, 127004 (2009).
 - ⁴⁷ R. T. Gordon, H. Kim, N. Salovich, R. W. Giannetta, R. M. Fernandes, V. G. Kogan, T. Prozorov, S. L. Budko, P. C. Canfield, M. A. Tanatar, and R. Prozorov, Phys. Rev. B **82**, 054507 (2010).
 - ⁴⁸ H. Kim, R. T. Gordon, M. A. Tanatar, J. Hua, U. Welp, W. K. Kwok, N. Ni, S. L. Budko, P. C. Canfield, A. B. Vorontsov, and R. Prozorov, Phys. Rev. B **82**, 060518(R) (2010).
 - ⁴⁹ Y. Zuev, M. S. Kim, and T. R. Lemberger, Phys. Rev. Lett. **95**, 137002 (2005).
 - ⁵⁰ D. J. Scalapino, S. R. White, S. C. Zhang, Phys. Rev. Lett. **68**, 2830 1992.
 - ⁵¹ D. J. Scalapino, S. R. White, S. C. Zhang, Phys. Rev. B **47**, 1995 1993.
 - ⁵² W.-F. Tsai, Y.-Y. Zhang, C. Fang, and J. Hu, Phys. Rev. B **80**, 064513 (2009).
 - ⁵³ T. Hanaguri, S. Niitaka, K. Kuroki, and H. Takagi, Science **328**, 474 (2010).
 - ⁵⁴ W.-Q. Chen and F.-C. Zhang, Phys. Rev. B **83**, 212501 (2011).